Pulsed nuclear magnetic resonance and nuclear spin dynamics in AlP†

Y. S. Hwang* and R. E. Norberg
Department of Physics, Washington University, St. Louis, Missouri 63130
(Received 10 June 1976)

Pulsed-nuclear-magnetic-resonance measurements are reported in powdered AlP. Measurements of the second moment of ^{31}P indicate that the dominant ^{31}P-^{27}Al interaction is 20% smaller than the calculated dipolar value. The reduction is interpreted in terms of an interference effect of the pseudodipolar interaction. A broadening of the ^{27}Al resonance is observed and found to arise from the first-order quadrupolar interaction. Nuclear spin-lattice relaxation of Al^{31}P is studied at 4.2, 78, and 300 K. Paramagnetic centers appear to be responsible for relaxing the ^{31}P nuclei at the higher temperatures. A rotating-frame multiple-pulse double-resonance experiment is used to study the evolution of the ^{31}P magnetization along the effective field under the simultaneous irradiation of a second ^{27}Al resonant rf field. A cross-relaxation model adopted can be used to describe one of the results reported in earlier rotating-sample experiments on AlP.

I. INTRODUCTION

Recent studies of III-V compounds have included nuclear-magnetic-resonance[1-3] (NMR) and nuclear-acoustic-resonance[4] (NAR) measurements of indirect nuclear exchange,[5-7] quadrupolar interactions,[8] and pseudodipolar interactions.[6] In general, the quadrupolar interaction and the indirect exchange interaction between unlike spins have broadening effects on the NMR lines. However, the pseudodipolar interaction can have a narrowing effect[2,3] if there is a p character of the electronic wave function in the solid. III-V compounds containing phosphorous seem to be characterized by a predominantly p character in the valence band and a large density of p states in the conduction band.[9]

Effects of the pseudodipolar interaction have been reported in[2] InP and GaAs.[3] AlP therefore appears to be an interesting system in which to search for electron-coupled interactions. AlP is a system with two abundant nuclear species and crystallizes in the zinc-blende lattice.[10] ^{31}P has spin $I=\frac{1}{2}$ and is free of quadrupole effects. ^{27}Al has spin $S=\frac{5}{2}$ and a quadrupole moment.

Previous NMR experiments on AlP have exhibited another interesting characteristic. Room-temperature experiments on rapidly rotating samples have been reported[11] on several compounds including powdered AlP. It was reported that the spin-lattice relaxation time of ^{31}P $[T_{1P}(\omega)]$ in AlP increased as the sample rotation frequency was increased. In the case of AlP, however, $T_{1P}(\omega)$ levelled off at the rotationally invariant spin-lattice relaxation time of ^{27}Al. On the other hand, in the static case the spin-lattice relaxations of ^{31}P and ^{27}Al in AlP proceeded independently. A stochastic spin-diffusion theory was unable to interpret the apparent cross-relaxation plateau in the curve $T_{1P}(\omega)$ vs ω.

In the present work, a multiple-pulse double-resonance (MPDR) method, which combines the characteristics of the multiple-pulse[12-14] and double-resonance[15] techniques, is used to produce a significant cross relaxation between ^{31}P and ^{27}Al in the rotating frame. A proposed cross-relaxation model can be used to describe the two extreme cases in the previously reported rotating-sample experiments on AlP.

II. PULSED NMR IN AlP

A. Experimental details

Pulsed NMR experiments were performed on ^{31}P at 15 MHz and on ^{27}Al at 9 MHz. For ^{31}P resonances, a single transmitter and receiver coil was used to produce a 90° pulse of duration 5.8 μsec. For ^{27}Al resonances, two crossed coils were used as transmitter and receiver coils, respectively. The crossed-coil system produced a 90° pulse of duration 28 μsec. Most measurements were performed at 78 K.

The powdered AlP used for the present work was purchased from Alfa Inorganics Inc. The impurity content was determined by a spectrographic analysis and is shown in Table I.

Low temperatures were obtained by directly immersing the sample, contained in a glass sample container, into the cryogenic fluid.

B. Second-moment measurements in AlP

1. Second moment from the free induction decay (FID)

The second moment $\langle\Delta\omega^2\rangle$ of the resonance line can be determined from the second derivative of the[16] FID $G(t)$ at $t=0$. One has

$$\langle\Delta\omega^2\rangle = -\left(\frac{d^2G(t)}{dt^2}\right)_{t=0}\Big/G(0)\,. \tag{1}$$

Figure 1 shows a semilogarithmic plot of the ^{31}P FID signal amplitude at 78 K as a function of the square of time. No temperature dependence

TABLE I. Spectrographic analysis of the AlP sample. [a]

Element	Concentration (at. %)
Iron	0.01–0.1
Silicon	0.03–0.3
Vanadium	Not detected
Magnesium	0.01–0.1
Copper	0.001–0.01
Maganese	0.001–0.01
Zinc	0.003–0.03
Sodium	0.001–0.01
Tin	0.001 [b]
Nickel	0.001 [b]
Lead	0.001–0.01

[a] The analysis was provided by Industrial Testing Laboratories, Inc., St. Louis, Mo.
[b] Less than.

was observed for the second moment of Al ^{31}P at the temperatures 300, 78, and 4.2 K.

The straight line in Fig. 1 corresponds to a Gaussian FID $G(t) = G(0)e^{-at^2}$. The second moment can be determined from the slope of the straight line with the result

$$\langle \Delta H^2 \rangle = 2a/\gamma^2_{^{31}\mathrm{P}} = 2.84\ \mathrm{G}^2 . \tag{2}$$

2. *Second moment from solid echoes*

a. 90-τ-90$_{90}$ sequence. Powles and Strange[17] have demonstrated that solid echoes can be used to achieve zero time resolution in pulsed NMR. The decay of the transverse magnetization following a 90-τ-90$_{90}$ pulse sequence has been calculated by Mansfield,[18] who showed that the second moments of the like and the unlike spins can be determined separately. The normalized results are

$$R''(\tau,\tau) = -\left(\frac{d^2R(t',\tau)}{dt'^2}\right)_{\tau'=\tau} = (\langle \Delta\omega^2 \rangle_{II} + \langle \Delta\omega^2 \rangle_{IS}) - \Delta_{4\epsilon}\tau^2 \tag{3}$$

and

$$R(\tau,\tau) = 1 - \langle \Delta\omega^2 \rangle_{IS}\tau^2 \tag{4}$$

for small τ. Here $R''(\tau,\tau)$ is the second time derivative of the echo signal evaluated at the echo maximum. $\langle \Delta\omega^2 \rangle_{II}$ and $\langle \Delta\omega^2 \rangle_{IS}$ are the respective second moments in sec^{-2} for the like and unlike spins and $\Delta_{4\epsilon}$ is a quantity related to the fourth moment of the resonance line.[18]

For $\tau \geq 40$ μsec, Fig. 2 shows a plot of $R''(\tau,\tau)$ as a function of τ^2 at 78 K. The straight line in Fig. 2 is a least-squares fit to the data plotted. The second moment is determined from the intercept of Fig. 2. The result is

$$\langle \Delta H^2 \rangle_{II+IS} = 2.85\ \mathrm{G}^2 . \tag{5}$$

For $\tau < 40$ μsec and from the τ^2 dependence of the echo signal, one obtains

$$\langle \Delta H^2 \rangle_{IS} = 2.20\ \mathrm{G}^2 . \tag{6}$$

b. 90-τ-180$_{90}$ sequence. Engelsberg and Norberg[2] derived an expression for the echo signal after a 90-τ-180$_{90}$ sequence. The sequence could be used to determine $\langle \Delta\omega^2 \rangle_{II}$ independently. The result is

$$R(\tau,\tau) \simeq 1 - [2(\tau)^2/2!]\langle \Delta\omega^2 \rangle_{II} \tag{7}$$

for small τ. From the $(2\tau)^2$ dependence of the

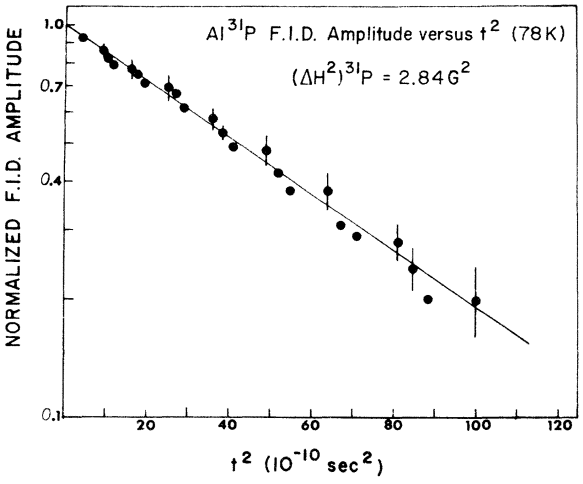

FIG. 1. Al ^{31}P FID amplitude as a function of t^2.

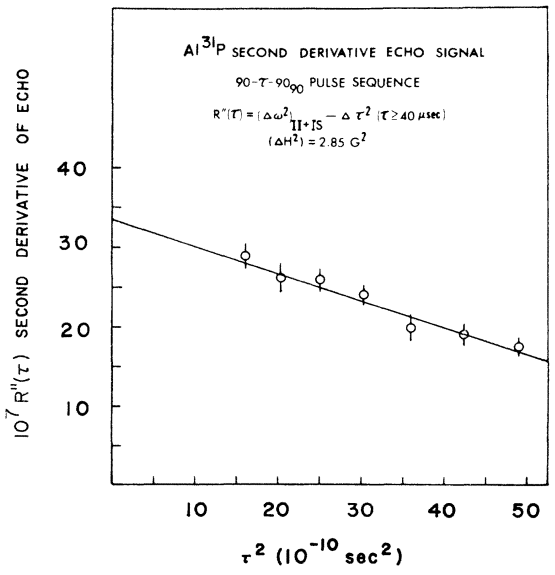

FIG. 2. Second derivative of the normalized ^{31}P echo signal as a function of the square of the pulse separation for a 90-τ-90$_{90}$ pulse sequence.

TABLE II. Comparison between theoretical and experimental second moments.

Calculated (G^2)	Experimental (G^2) (78 K)
$\langle\Delta H^2\rangle_{\text{total}}^{^{31}\text{P},\text{dipolar}} = 3.55$	$\langle\Delta H^2\rangle_{\text{total}}^{^{31}\text{P},\text{FID}} = 2.84$
	$\langle\Delta H^2\rangle_{IS}^{^{31}\text{P},\text{echo}} = 2.85$
$\langle\Delta H^2\rangle_{IS}^{^{31}\text{P},\text{dipolar}} = 3.28$	$\langle\Delta H^2\rangle_{IS}^{^{31}\text{P},\text{echo}} = 2.2$
$\langle\Delta H^2\rangle_{II}^{^{31}\text{P},\text{dipolar}} = 0.27$	$\langle\Delta H^2\rangle_{II}^{^{31}\text{P},\text{echo}} = 0.29$

Al ^{31}P echo signal, one obtains

$$\langle\Delta H^2\rangle_{II} = 0.29\,G^2, \tag{8}$$

which is comparable to the theoretical dipolar value $\langle\Delta H^2\rangle = 0.27$ G^2. Table II contains a summary of various experimental second moments and also shows the calculated dipolar values.[19] The parameters used for the calculation are $\sum_k r_{jk}^{-6} = 115.6a^{-6}$ for like spins, $\sum_{k'} r_{jk'}^{-6} = 660.5a^{-6}$ for unlike spins and $a = 5.42$ Å for AlP. From Table II, one sees that the second moment $\langle\Delta H^2\rangle^{^{31}\text{P}}$ determined from the FID is close to that obtained from the solid echo. The sum of $\langle\Delta H^2\rangle_{II}$ and $\langle\Delta H^2\rangle_{IS}$ is only in reasonable agreement with that determined from the FID and solid echo. Since the dipolar interaction between unlike spins makes the major contribution to the total second moment and since the total second moment determined from the FID is in good agreement with that determined from the solid echo, one estimates $\langle\Delta H^2\rangle_{IS} = 2.56$ G^2 from Eqs. (5) and (8). This value will be used for later discussion.

C. Results and discussion

From Table II, one sees that the total second moment is about 20% smaller than the calculated value. Since no temperature dependence was observed for the second moment, motional narrowing probably can be excluded. Exchange narrowing can also be ruled out since the $90\text{-}\tau\text{-}180_{90}$ experiment does not show any evidence of this effect. Also, since the like spins make a minor contribution to the total second moment, it would not be anticipated that the like-spin interaction could produce such a narrowing effect. Therefore, the reduction in the second moment is assumed to arise from the pseudodipolar interaction. The same kind of pseudodipolar interference effect has been reported[2,3,20] in TlCl, InP, and GaAs.

Let us define the exchange and pseudodipolar constants between unlike spins as $A_{jk'}^{IS}$ and $B_{jk'}^{IS}$, respectively. Following the treatment in Ref. 2, one obtains for a powder, the mutual second moment of the resonant I spins including both exchange and pseudodipolar interactions:

$$\langle\Delta\omega^2\rangle_{IS}^{I} = \langle\Delta\omega^2\rangle_{IS,\,\text{dipolar}}^{I} + \tfrac{1}{3}S(S+1)\sum_{k'}(A_{jk'}^{IS})^2 + \tfrac{4}{15}S(S+1)\sum_{k'}\left((B_{jk'}^{IS})^2 + \frac{2\gamma_I\gamma_S\hbar B_{jk'}^{IS}}{r_{jk'}^3}\right). \tag{9}$$

Substituting in Eq. (9) the calculated $\langle\Delta\omega^2\rangle_{IS,\,\text{dipolar}}^{^{31}\text{P}}$, the experimental $\langle\Delta\omega^2\rangle_{IS,\text{dipolar}}^{^{31}\text{P}}$ and using the nearest-neighbor approximation for electron-coupled interactions,[6] a quadratic equation is obtained, which has real roots of $B_{jk'}^{IS}$ only if

$$|A_{jk'}^{IS}| \leq 4.8\times10^3\ \text{sec}^{-1}. \tag{10}$$

The roots of $B_{jk'}^{IS}$ corresponding to Eq. (10) are

$$-11.5\times10^3 \leq B_{jk'}^{IS} \leq -0.8\times10^3\ \text{sec}^{-1}. \tag{11}$$

Equations (10) and (11) obviously demonstrate a negative sign of the pseudodipolar interaction constant, which is deduced semiempirically. From Eq. (9), the value of $|A_{jk'}^{IS}|$ which minimizes the ratio $|B_{jk'}^{IS}/A_{jk'}^{IS}|$ is $|A_{jk'}^{IS}| = 2.3\times10^3$ sec^{-1}. The corresponding value of $|B_{jk'}^{IS}|$ is 1.4×10^3 sec^{-1}. The second moment results thus imply

$$|B_{jk'}^{IS}/A_{jk'}^{IS}| \geq 0.6. \tag{12}$$

The finite value of B implied by Eq. (12) indicates that the electronic wave function in the solid has a non-S character.[6]

A localized bond model can be used to estimate the electron-coupled interactions for solids with a partially covalent bond. AlP, however, is more covalent than ionic. Attempts to discuss our results by this model can lead only to tentative conclusions.

The model was first introduced by Yosida and Moriya[21] to calculate the electron-coupled interactions in ionic crystals. The same model was also used by Bloembergen and Sorokin[22] and Clough and Goldburg[20] in their studies of cesium halides and thallium chloride, respectively.

A more refined calculation of electron-coupled interactions, which included the admixture of S and P characters of the electronic states, was given by Engelsberg.[23] His results for both the exchange (A_{ij}^{IS}) and pseudodipolar (B_{ij}^{IS}) interaction constants have been rechecked to be[24]

$$A_{ij}^{IS} = C\left(\tfrac{128}{9}\pi^2 A_{si}A_{sj} + \tfrac{16}{25}A_{pi}A_{pj}\right), \tag{13a}$$

$$B_{ij}^{IS} = -C\left[\tfrac{8}{25}A_{pi}A_{pj} + \tfrac{32}{15}\pi(A_{pi}A_{sj} + A_{pj}A_{si})\right], \tag{13b}$$

with

$$C = \mu_B^2\gamma_i\gamma_j\hbar\lambda(a_{si}a'_{si} + a_{pi}a'_{pi})(a_{sj}a'_{sj} + a_{pj}a'_{pj}), \tag{13c}$$

$$A_{pi} = a_{pi}\, a'_{pi} \langle r_i^{-3} \rangle_p , \quad A_{si} = a_{si}\, a'_{si} |\, \phi^2_{si}(0)| , \quad (13d)$$

$$A_{pj} = a_{pj}\, a'_{pj} \langle r_j^{-3} \rangle_p , \quad A_{sj} = a_{sj}\, a'_{sj} |\, \phi^2_{sj}(0)| , \quad (13e)$$

where a_{si}, a_{pi}, etc., are the coefficients of the atomic orbitals for S and P character, respectively, and λ measures the degree of covalency of the bond. $\langle r^{-3} \rangle$ is the average value of r^{-3} for the atomic P orbital and $|\phi^2_S(0)|$ is the electronic wave density for the S electron at the nucleus.

An interesting consequence of the simple localized model is that it predicts a negative sign of the pseudodipolar interaction constant, qualitatively in agreement with our experimental result, and gives a ratio of $|B^{IS}/A^{IS}|$ which is independent of the degree of covalency. It also shows that the pseudodipolar interaction vanishes for purely S electronic wave functions.

Equations (12), (13a), and (13b) exclude the possibility of the same ratio of P to S character for the electronic wave function around each type of atom[23,24] in AlP. One can obtain reasonable values for both A^{IS} and B^{IS} if one assumes that the wave functions around phosphorous are tetrahedral and assigns a 65% P character and 35% S character to the excited states around aluminum atoms. From Eqs. (12) and (13), one then obtains[24] $A^{IS} = 1.5 \times 10^3$ sec^{-1} and $B^{IS} = -0.9 \times 10^3$ sec^{-1}, compared to our semiempirical conditions, Eqs. (10) and (11). There is a tendency for shifts of the wave functions,[25] which may lead to a change in the degree of covalency. However, the ratio of $|B^{IS}/A^{IS}|$, as predicted by the localized bond model is independent of the degree of covalency.

Recently, using a similar perturbation-theory technique, Huang *et al.*[26,27] have discussed calculations of the pseudodipolar and exchange interaction constants and other applications based on a two bond orbital model. The derived ratios of the pseudodipolar to exchange interaction constants are the same as Eqs. (13) if we set $a_s = a_{s'} = \frac{1}{2}$ and $a_p = a_{p'} = \frac{1}{2}\sqrt{3}$, which are the sp^3 hybrid conditions used in their calculations. In Ref. 27 the derived ratios for AlP of B/P_{dd}, A/P_{dd}, and B/A are 0.0451, 0.296, and 0.152, respectively, without taking into account the overlap terms and electron correlation effects. When such terms are included in the calculations, the values of B and A are enhanced and increase the ratios B/P_{dd} and A/P_{dd} to the values 0.102 and 0.684, respectively, while the ratio of B/A is unchanged.

The second-moment determinations in the present work indicate that the ratio of the pseudodipolar exchange interaction constants, lies between 0.17 to 2.4. Equation (12) seems to exclude the possibility of the lower ratios. Using our modified values of $|B| = 0.9 \times 10^3$ sec^{-1} and $|A| = 1.5 \times 10^3$ sec^{-1}, the ratios of B/P_{dd} and A/P_{dd} for AlP are, respectively, 0.15 and 0.25 while the ratio of B/A is 0.6.

D. Second moment of ^{27}AlP

Aluminum has spin $S = \frac{5}{2}$ and a quadrupole moment. The quadrupolar interaction with random defects then is expected to broaden the aluminum resonance line. For high concentration of substitutional impurities, Rhoderick[28,29] and Oliver[30] found that a loss in intensity of the NMR signal in semiconductors arose from the quadrupolar interaction between the nuclei and the electric field gradients (efg) produced by ionized impurities. In the following discussion, an efg of cylindrical symmetry has been assumed.

In the present work, the second moment of ^{27}AlP will be shown to be 40% larger than the calculated dipolar value. This additional broadening will be identified as arising from unresolved first-order quadrupolar broadening and the second-order quadrupole effect will be shown to be negligible.

The first-order quadrupolar shift for $m \leftrightarrow (m-1)$ is[1,8,31]

$$\Delta\nu_m = [3(2m-1)eQ/4S(2S-1)h]V_{jzz} ,$$

with $V_{jzz} = \partial^2 V/\partial z^2$, the field gradient component at the nucleus along the external magnetic field. Q is the quadrupole moment. For $S = \frac{5}{2}$, the linewidth, in the case of unresolved first-order quadrupole broadening from random field gradients, will be given approximately by

$$\Delta\nu \sim 4\nu_Q , \quad (14a)$$

with

$$\nu_Q = \tfrac{3}{2}[eQ/S(2S-1)h]V_{jzz} . \quad (14b)$$

The second-order quadrupole effect will become important, when

$$\nu_Q^2/\nu_0 \sim \nu_D , \quad (15)$$

where ν_0 is the resonant frequency of the resonant spins and ν_D is the dipolar linewidth.

From the discussion in Sec. II C, it seems reasonable to assume that both an S and P character exists for the electronic wave functions around the aluminum atoms. One therefore includes both exchange and pseudodipolar interactions in the aluminum second-moment expression. Following the notations of Sundfors[4] and Hester *et al.*,[3] the second moment for a powder can be written

$$\langle \Delta\omega^2 \rangle^S = \langle \Delta\omega^2 \rangle_D^{SS} + \langle \Delta\omega^2 \rangle_D^{SI} + \langle \Delta\omega^2 \rangle_{\rm PD}^{SS} + \langle \Delta\omega^2 \rangle_{\rm PD}^{SI} + \langle \Delta\omega^2 \rangle_E^{SI} + \langle \Delta\omega^2 \rangle_{\rm quad} , \quad (16a)$$

with

$$\langle \Delta\omega^2 \rangle_D^{SS} = \tfrac{3}{5} S(S+1)\gamma_S^4 \hbar^2 \sum_k r_{jk}^{-6} , \quad (16b)$$

$$\langle \Delta\omega^2 \rangle_{PD}^{SS} = \tfrac{3}{5} S(S+1) \sum_k (2\gamma_S^2 \hbar B_{jk} r_{jk}^{-3} + B_{jk}^2), \tag{16c}$$

$$\langle \Delta\omega^2 \rangle_{D}^{SI} = \tfrac{4}{15} I(I+1)\gamma_S^2 \gamma_S^2 \hbar \sum_{k'} r_{jk'}^{-6}, \tag{16d}$$

$$\langle \Delta\omega^2 \rangle_{PD}^{SI} = \tfrac{4}{15} I(I+1) \sum_{k'} (2\gamma_I \gamma_S \tilde{B}'_{jk'} r_{jk'}^{-3} + \tilde{B}'^2_{jk'}), \tag{16e}$$

$$\langle \Delta\omega^2 \rangle_{E}^{SI} = \tfrac{1}{3} I(I+1) \sum_{k'} \tilde{A}'^2_{jk'}, \tag{16f}$$

$$\langle \Delta\omega^2 \rangle_{quad} = \tfrac{9}{5}[4S(S+1) - 3]\frac{A^2}{\hbar^2} \sum_j (V_{jzz}^2). \tag{16g}$$

$B_{jk'}$, $\tilde{B}_{jk'}$, $\tilde{B}'_{jk'}$ are the pseudodipolar (PD) constants for like spins S, like spins I, and unlike spins, respectively. Similar notations are employed for the exchange (E) constants A'_{jk}. "quad" stands for the quadrupolar interaction and $A = eQ/4S(2S-1)$.

Figure 3 shows a semilogarithmic plot of the observed FID signal amplitude of ^{27}AlP as a function of the square of time. No temperature dependence was observed at 300, 78, and 4.2 K. Defining $G(t) = G(0)e^{-bt^2}$, the second moment is found from the slope of the straight line in Fig. 3:

$$\langle \Delta H^2 \rangle_{FID}^{Al} = 2b/\gamma_{Al}^2 = 2.71\ \mathrm{G}^2. \tag{17}$$

The calculated dipolar value is from Eqs. (16b) and (16d),

$$\langle \Delta H^2 \rangle_{calc}^{Al} = 1.97\ \mathrm{G}^2. \tag{18}$$

Kambe and Ollom[32] derived the second moment of the dipolar-broadened central line when the quadrupolar coupling is so strong that the central component is well resolved from the satellites. Their results for the second moment included both dipolar and exchange interactions. To evaluate the exchange constant between like spins for the Kambe and Ollom formula, one can write Anderson's exchange constant as[4]

$$A_{jk} = a_{jk}\gamma_j\gamma_k \hbar r_{jk}^{-4}, \tag{19a}$$

with

$$a_{jk} = (8/9\pi)\gamma_e^2 \Omega^2 \epsilon_j \psi_j^2(0) \epsilon_k \psi_k^2(0) m^*, \tag{19b}$$

where Ω is the atomic volume and $\epsilon_j = [\psi_j(0)_{hole} \times \psi_j^*(0)_{electron}]/[\psi_j^2(0)]_{atom}$. In Ref. 4, the values of the wave-function density $\epsilon_j\psi_j^2(0)$ were obtained from semiempirical values A_{jk} and $\tilde{A}'_{jk'}$ and were proportional to the atomic number of nucleus j, as predicted by the Fermi-Segrè formula.[33]

If one assumes that Eqs. (19) apply to AlP, and the wave-function density is taken to be proportional to the atomic number, one can estimate the exchange interaction constant for AlP from that of InP. The result is

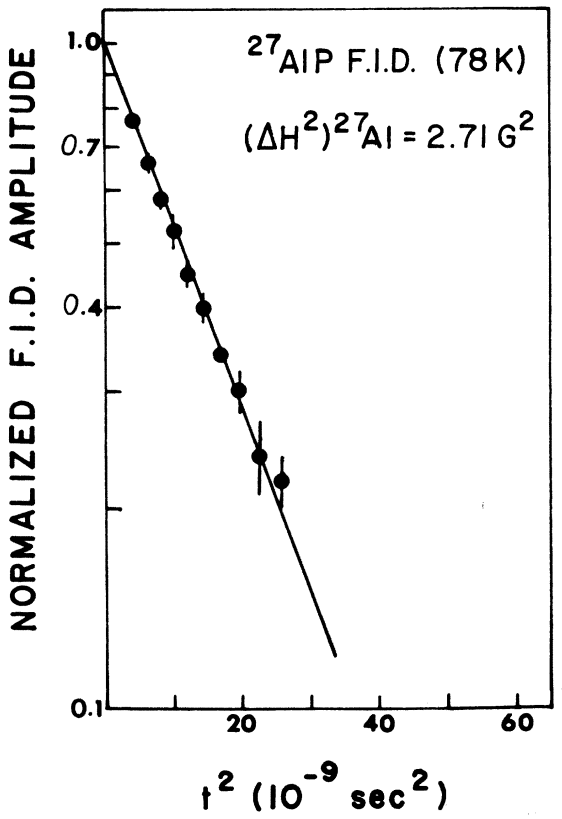

FIG. 3. ^{27}AlP FID amplitude as a function of t^2.

$$A'_{AlP} = \tilde{A}'_{InP}\gamma_{Al} a_{AlP}^2 Z_{Al}/\gamma_{In} a_{InP}^2 Z_{In} = 0.89 \times 10^3 \mathrm{sec}^{-1}, \tag{20}$$

with $\tilde{A}'_{InP} = 3.3 \times 10^3$ sec^{-1}.[23] a_{AlP}, a_{InP} are the respective lattice constants and Z is the atomic number. To find $A_{Al\,Al}$, one uses Eqs. (19) to obtain

$$A_{Al\,Al} = \tilde{A}'_{AlP}\gamma_{Al} Z_{Al}(a_{Al\text{-}P})^4/\gamma_P Z_P (a_{Al\text{-}Al})^4 = 0.07 \times 10^3\ \mathrm{sec}^{-1}, \tag{21}$$

with $a_{Al\text{-}P} = 2.35$ Å and $a_{Al\text{-}Al} = 3.84$ Å, where $a_{Al\text{-}P}$ and $a_{Al\text{-}Al}$ are the distances from the aluminum to the nearest phosphorous atom and to the nearest aluminum atom, respectively. Since the electron-coupled interactions are short range, only the nearest neighbors for like spins are included in the calculation of the exchange terms in the second moment. Kambe and Ollom's[32] formula and Eqs. (20) and (21) give

$$\langle \Delta H^2 \rangle_D^S = 1.57\ \mathrm{G}^2 \tag{22a}$$

for like and unlike spins, and

$$\langle \Delta H^2 \rangle_D^S = 1.71\ \mathrm{G}^2 \tag{22b}$$

for semilike and unlike spins. A compromise value between Eqs. (22) could be taken. Comparing Eqs. (17) and (22), one concludes that the observed second moment does not arise from the dipolar-broadened central component with all satellites well resolved from it.

From Eq. (9), one had

$$\langle\Delta\omega^2\rangle^{IS} = \langle\Delta\omega^2\rangle_D^{IS} + \langle\Delta\omega^2\rangle_E^{IS} + \langle\Delta\omega^2\rangle_{\rm PD}^{IS}, \tag{23}$$

with

$$\langle\Delta\omega^2\rangle_E^{IS} = \tfrac{1}{3}S(S+1)\sum_{k'}(\tilde{A}'_{jk'})^2. \tag{24}$$

Equations (20) and (24) give

$$\langle\Delta\omega^2\rangle_{E,^{31}{\rm P}}^{IS} = -0.09\times10^8\ {\rm sec}^{-2}, \tag{25}$$

and Eq. (23) gives

$$\langle\Delta\omega^2\rangle_{{\rm PD},^{31}{\rm P}}^{IS} = -0.94\times10^8\ {\rm sec}^{-2}. \tag{26}$$

If one assumes that the electron-coupled interaction constants are the same between *IS* and *SI*, then

$$\langle\Delta\omega^2\rangle_{E,^{27}{\rm Al}}^{SI} = 0.01\times10^8\ {\rm sec}^{-2}, \tag{27}$$

$$\langle\Delta\omega^2\rangle_{{\rm PD},^{27}{\rm Al}}^{SI} = -0.09\times10^8\ {\rm sec}^{-2}, \tag{28}$$

and $\langle\Delta\omega^2\rangle_{{\rm PD},^{27}{\rm Al}}^{SS}=0$ for the nearest-neighbor approximation. Equation (16a) gives

$$\langle\Delta\omega^2\rangle_{\rm quad} = 0.44\times10^8\ {\rm sec}^{-2}. \tag{29}$$

Equating Eq. (29) to Eq. (16g), one finds

$$\frac{1}{N}\sum_j V_{jzz}^2 = 26.51\times10^{22}\ {\rm esu/cm}^2. \tag{30}$$

From Eq. (14b),

$$\nu_Q^2 \simeq \left(\frac{3eQ}{2S(2S-1)h}\right)^2\frac{1}{N}\sum_j V_{jzz}^2 = 7\times10^5\ {\rm Hz}^2 \tag{31}$$

or

$$\nu_Q = 8.4\times10^2\ {\rm Hz}. \tag{32}$$

One could also find

$$\nu_Q^2/\nu_0 = 7.2\times10^2\ {\rm Hz}$$

and

$$\Delta\nu_{\rm expt} \simeq 3.6\times10^3\ {\rm Hz}, \tag{33a}$$

$$\Delta\nu_{D,{\rm calc}} = 3.1\times10^3\ {\rm Hz}, \tag{33b}$$

where one has assumed $\frac{1}{4}\delta H^2 = \langle\Delta H^2\rangle$ holds for the Gaussian. One therefore has

$$\nu_Q^2/\nu_0 < \Delta\nu_{D,{\rm calc}},$$

and the second-order quadrupole effect is not important in broadening the aluminum resonance line. Also, Eqs. (32) and (33a) give

$$\Delta\nu_{\rm expt} \sim 4\nu_Q,$$

which is just the condition for the first-order quadrupolar broadening in random EFG, Eq. (14a).

Therefore, the 40% additional line broadening of ^{27}Al in powdered AlP probably arises from first-order quadrupolar interaction in random EFG.

E. Spin-lattice relaxation in Al ^{31}P

The purpose of this section is to summarize some observed features of nuclear relaxation of ^{31}P in AlP rather than to give a comprehensive study of the relaxation mechanisms. The latter would require more detailed information about the impurities in our sample than is available.

Measurements of T_1 were performed by a 90°-90° pulse sequence. The recovery of the ^{31}P magnetization was found to be nonexponential at 4.2, 78, and 300 K (Figs. 4–6). A transition region in the time dependence becomes more pronounced as the temperature is lowered.

^{31}P has spin $I=\frac{1}{2}$ and is free of quadrupolar interaction. The field dependence of T_1 of ^{31}P in AlP,[11] seems to exclude possible relaxation arising from conduction electrons.[34,35] The increase in T_1 as temperature is lowered also rules out relaxation arising from the bound states of impurities.[34,36] The T_1 values, determined by approximating the last portion in the magnetization recovery by an exponential, are shown as a function of temperature in Fig. 7.

In solids in which there is no rapid atomic dif-

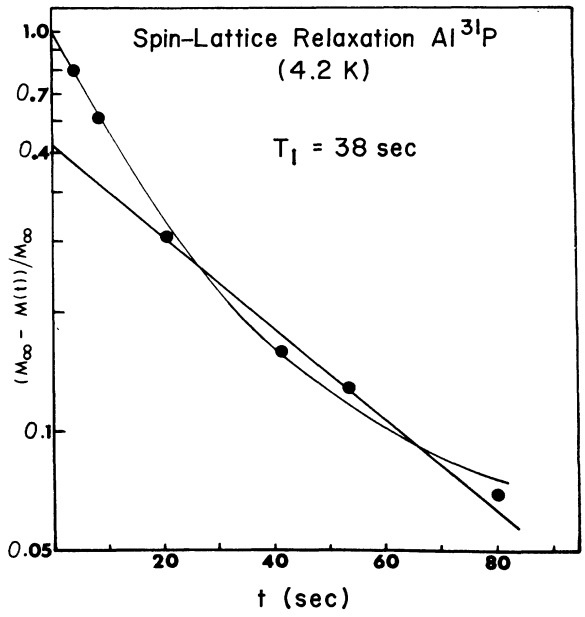

FIG. 4. Fractional recovery of the ^{31}P magnetization in AlP at 4.2 K.

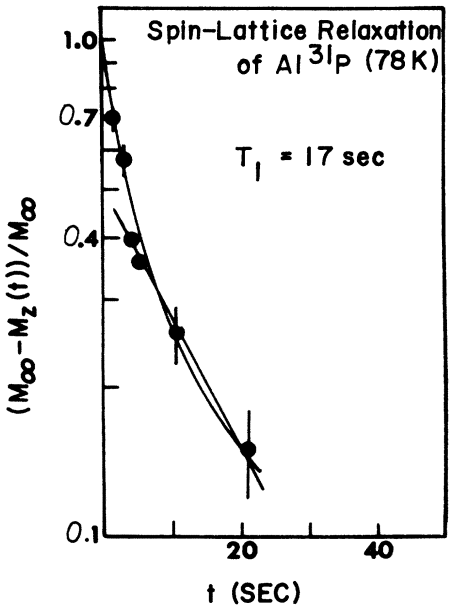

FIG. 5. Fractional recovery of the ^{31}P magnetization in AlP at 78 K.

fusion, spin diffusion to paramagnetic centers can play an important role in nuclear relaxation. A typical expression for T_1 can be written [37,38]

$$T_1 = (1/4\pi NDb) I_{-3/4}(x)/I_{3/4}(x)\,, \tag{34}$$

where $I_{\mp 3/4}(x)$ are modified Bessel functions. N, b, and x have their usual meanings. x is proportional to the square of the ratio of the pseudopotential radius b,[39] to the diffusion barrier δ_i. Where $\delta_i = \delta$ for $b \gg \delta$ and $\delta_i = \delta' = (b\delta)^{1/2}$, when $b \ll \delta$.[40] D is the spin-diffusion constant and is given by[41]

$$D = \frac{\pi}{120}\gamma_I^4 \hbar^2 T_{2P} \sum_j{}' r_{ij}^{-4}\,, \tag{35a}$$

where summation is over all like nuclei j. The condition for Eq. (34) is

$$a' \ll \max(b, \delta_i) \ll R\,, \tag{35b}$$

where R is the radius of a sphere around one magnetic ion. Equation (34) can be reduced to the two conventional cases of spin-diffusion limited (SDL) and rapid spin-diffusion (RSD) relaxation[37,39,41,42] when the ratio b/δ_i is large or small, respectively.

Blumberg[42] found that, in the SDL case, the magnetization recovery after saturation will proceed via the direct relaxation only for a short time during which a $t^{1/2}$ dependence of the fractional magnetization recovery is expected. The initial slope of M_z/M_0 is[42]

$$m = \tfrac{4}{3}\pi^{3/4} N C^{1/2}\,. \tag{36}$$

The appearance of nonexponential behavior at small times in the magnetization recovery curves seems to exclude the possibility of relaxation in the RSD regime.[41,42] On the other hand, it is characteristic of relaxation by dilute paramagnetic centers.[42,43] A similar nonexponential recovery has been reported in $Zn_3{}^{31}P_2$ and Al ^{31}P and by Engelsberg[23] in one of his InP samples.

The results of a spectrographic analysis in Table I show many impurities. Two possibly abundant paramagnetic impurities will be considered here.

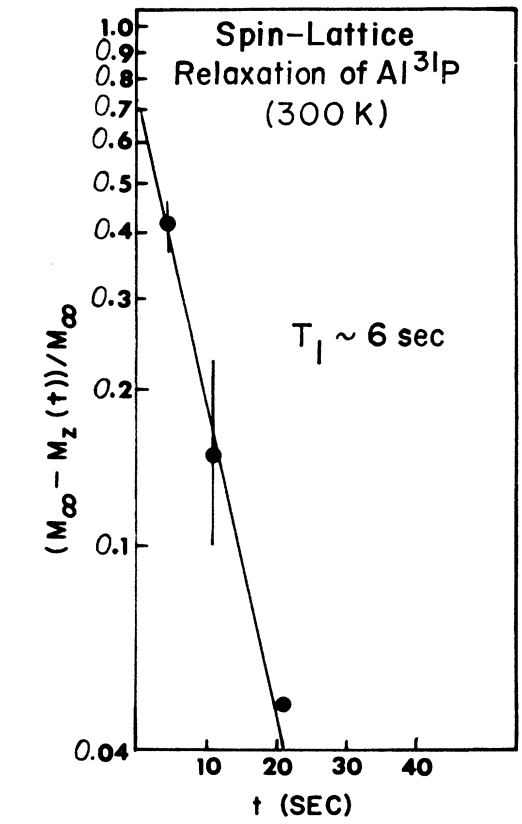

FIG. 6. Fractional recovery of the ^{31}P magnetization in AlP at 300 K.

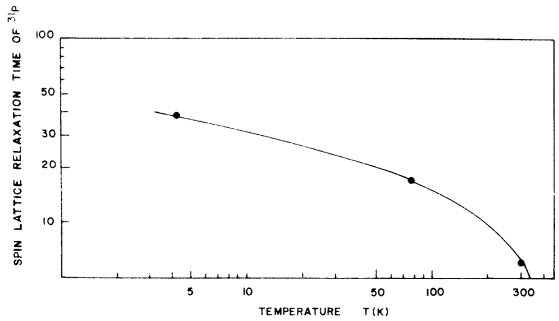

FIG. 7. Comparison of T_1 of ^{31}P in AlP at 300, 78, and 4.2 K.

TABLE III. Relaxation times and magnetization rates.

Temperature (K)	Calculated T_1 (sec)	Experimental T_1 (sec)	m_{expt}	m_{calc}
300	49	38	0.27	0.04
78	15	17		
4.2	3	$\lesssim 6$	0.29	0.15

From Fig. 7, one sees a small increase in T_1 as the temperature is lowered. This implies that $\tau \gg 10^{-8}$ sec. Moreover, T_1 at higher temperatures seems more temperature dependent than that at lower temperature. This may imply that at higher temperature the nuclear relaxation arises from the temperature-dependent spin-lattice interaction of the paramagnetic ion and at lower temperature, the nuclear relaxation is determined by the temperature-independent spin-spin interaction among the ions.

It can be shown[24] that iron impurities probably are not the ^{31}P relaxing agents. However, a reasonably consistent set of results can be obtained with 3×10^{18} Mn^{2+} ions per cm^3. Table III lists observed results and calculated values [from Eqs. (34) and (36)] for T_1 and m, where m is the slope of M_z/M_0 vs t, determined for $t \leq q$ sec. The lattice sums involved in the calculation of D were evaluated by adding the contributions of 16 shells of phosphorus atoms and approximating the contributions from more remote atoms by an integration over a uniform distribution. The calculated results for R, b, and δ_i satisfy Eq. (35). It is probable that the relaxation processes occur in a regime intermediate between the SDL and RSD limits. The nonexponential recovery of the magnetization suggests the SDL case. Generally $\delta' > 3b$ characterizes the RSD case.[37] The Mn^{2+} calculations yield δ' values of $2.6b$ (4.2 K), $1.7b$ (78 K), and $\sim 1b$ (300 K). There is better agreement between the calculated and observed m values at 300 K than at the lower temperature and one probably is closer to the SDL case at 300 K.

III. NUCLEAR-SPIN DYNAMICS IN AlP

Figure 8 shows some relevant excerpts of the previously published rotating sample experiments on AlP. Two features are to be noted: (i) In the static sample case, the spin-lattice relaxation of ^{31}P (T_{1P}) and that of ^{27}Al (T_{1Al}) proceed independently; (ii) $T_{1P}(\omega)$ increases with increasing mechanical rotation frequency ω and finally approaches the rotationally invariant T_{1Al}. It was concluded that T_{1P} and $T_{1P}(\omega)$ at small ω arose from the relaxation of the ^{31}P nuclei to the paramagnetic impurity centers via spin diffusion, where the spin-diffusion constant varied with the rotation frequency. However, the stochastic theory of spin diffusion presented was unable to explain the observed plateau at high rotation frequency in the curve of $T_{1P}(\omega)$ vs ω as shown in Fig. 8. It was suggested that some unspecified cross-relaxation mechanism was responsible for the equality of $T_{1P}(\omega)$ and T_{1Al} at large ω, but no convincing model was proposed. In order to help to understand the situation, a multiple-pulse double-resonance (MPDR) technique now has been used to simulate the mechanical rotation and to study the AlP cross-relaxation in the rotating frame. Under some reasonable assumptions, the limiting cases in the rotating sample experiments can be explained from the cross-relaxation model adopted here.

The MPDR experiment, which combines the characteristics of both multiple-pulse[12-14] and double-resonance[15] techniques, is used to induce a cross-relaxation phenomenon. The multiple-pulse technique can be viewed as an artificial line-narrowing mechanism,[12,13,44-46] whose effect is to prolong the FID by several orders of magnitude. This is analogous to the line-narrowing experiments produced by rapid mechanical rotation of the sample.[11] Some multiple-pulse effects can also

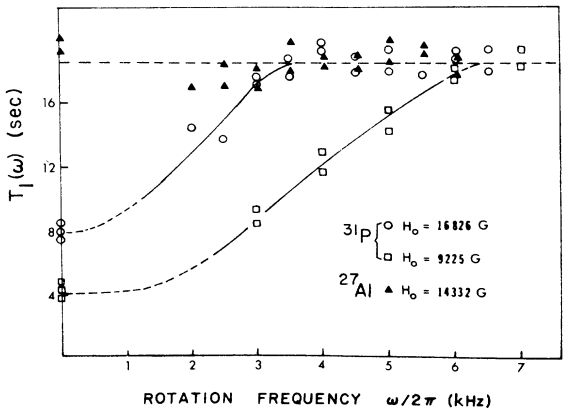

FIG. 8. Dependence of ^{31}P and ^{27}Al spin-lattice relaxation times in AlP on frequency of sample rotation (from Fig. 13 of Ref. 11).

be simulated by spin locking[15,47] the magnetization in long pulses of small amplitude.[2,48,49]

Nuclear magnetic double resonance was first proposed by Hartmann and Hahn[15] as a method for detecting weak nuclear magnetic resonances. Recently, many nuclear magnetic double-resonance experiments have been performed including studies of rare[50-55] and abundant[13,56-58] nuclei in solids.

In our multiple-pulse double-resonance experiment, a $90-\tau-90_{90}-2\tau\cdots$ pulse sequence[14,48] is applied to the resonant I spins (in our case ^{31}P) and a $\theta_{S,0}{}^\circ-\tau-\theta_{S,0}{}^\circ-2\tau-\theta_{S,0}{}^\circ-2\tau\cdots$ sequence simultaneously is applied to the resonant S spins (^{27}Al). The first pulse in the S-spins rf sequence is applied at the same initial time as the second pulse of the I-spin rf sequence. The response to both rf pulse sequences is studied as a function of the pulse-separation 2τ and the pulse width of the rf pulse of the S spins. The evaluation of the magnetization $M_{\bar{Z}}$ of the I spins is observed between pulses.

The relevant characteristics of the evolution of the $\bar{Z}$ component of the magnetization with $\bar{H}_{1S}=0$ and $\bar{H}_{1S}\neq 0$ are shown in Fig. 9 for some typical values of $\bar{H}_{1I}$. With $\bar{H}_{1S}=0$ [Fig. 9(a)], a sharp initial drop in the magnetization from its equilibrium value M_0 and an oscillation[49] of the order of $T'\sim 8\tau$ [Fig. 9(c)] were observed. Following the oscillation, the echo envelope decays monotonically. This is the phenomenon reported previously in the same type of multiple-pulse experiment on InP. A common spin temperature between the Zeeman and the cross-coupling terms is established at the end of the oscillation. With $\bar{H}_{1S}\neq 0$ [Fig. 9(b)], the echo envelope decay faster than with $\bar{H}_{1S}=0$. The oscillation becomes less obvious for large ratios of $t_{\omega S}/t_{\omega S,90^\circ}$. Here $t_{\omega S}$ is the pulse width of arbitrary duration for the S-spin rf field and $t_{\omega S,90^\circ}$ is a 90° pulse for the S spins. The reduction of the I magnetization is faster and more complete for larger ratios of $t_{\omega S}/t_{\omega S,90^\circ}$.

In the multiple-pulse experiments, the multiple-pulse sequence can be expanded in a Fourier series.[48] For a $90-\tau-90_{90}-2\tau\cdots$ sequence applied at the resonant frequency of the I spins, the zeroth component in a Fourier expansion is a rotating magnetic field of amplitude:

$$\bar{H}_{1I}=\pi/4\gamma_I\tau\,. \tag{37}$$

For an arbitrary pulse width, applied at the resonant frequency of the S spins,

$$\bar{H}_{1S}=(H_{1S}/2\tau)t_{\omega S}\,. \tag{38}$$

For 90° pulses applied to the S spins, one has

$$\bar{H}_{1S}=\pi/4\gamma_S\tau\,. \tag{39}$$

Here, H_{1I}, H_{1S} are the magnitudes of the rotating magnetic fields.

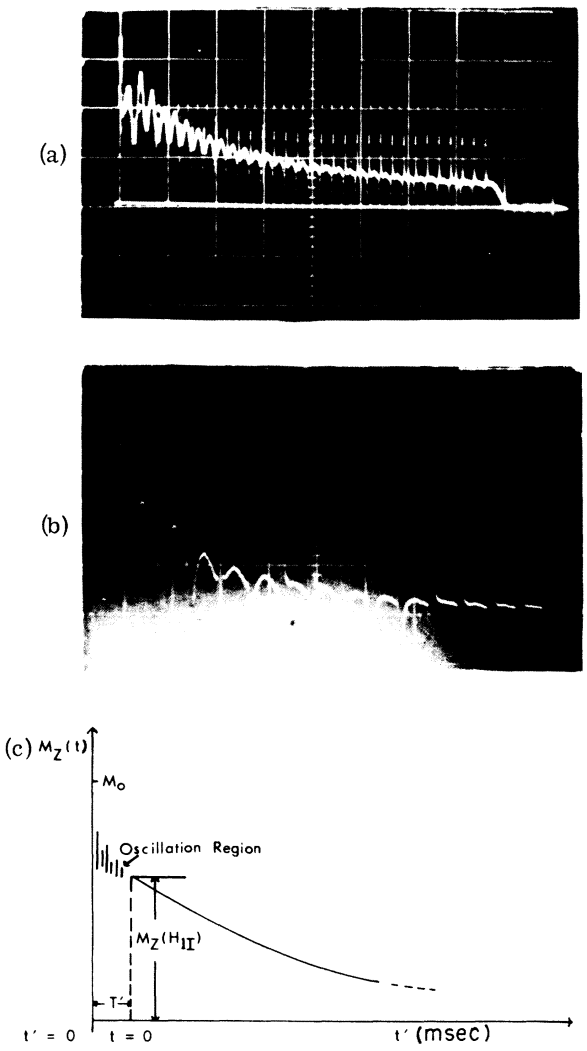

FIG. 9. (a) Oscilloscope photograph of train of solid echoes in the multiple-pulse single-resonance experiment ($\bar{H}_{1S}=0$). τ is 60 μsec and the sweep length is 5 msec. (b) Echo train in multiple-pulse double-resonance experiment ($\bar{H}_{1S}\neq 0$). τ is 60 μsec and the sweep length is 2 msec. (c) Sketch of the evolution of the magnetization $M_Z(\bar{H}_{1I})$ of the I spins for typical values of $\bar{H}_{1I}$.

Equations (37) and (39) give

$$\gamma_I\bar{H}_{1I}=\gamma_S\bar{H}_{1S}\,. \tag{40}$$

which is similar to the well-known Hartmann and Hahn[15] double-resonance condition at which the approach to equilibrium would be fastest and the destruction of the I magnetization due to the S spins would be a maximum.

The effect of the presence of two rf irradiations can be better understood if the density matrix of the spin system is transformed to two respective

rotating frames by the transformation

$$R = e^{i\omega_I I_z t} e^{i\omega_S S_z t},$$

where $\omega_I = \gamma_I H_0$, $\omega_S = \gamma_S H_0$ are the respective Larmor frequencies of the resonant I and S spins. The final relevant transformed Hamiltonian is

$$\begin{aligned} H_f^* &= H_{\bar{z}I}^* + H_{\bar{z}S}^* + H_{II}^* + H_{IS}^* \\ &= -\gamma_I \bar{H}_{1I} I_{\bar{z}} - \gamma_S \bar{H}_{1S} S_{\bar{z}} \\ &\quad + \sum_{k>j} (A_{jk}^I \tilde{I}_j \cdot \tilde{I}_k + B_{jk}^I I_{j\bar{z}} I_{k\bar{z}}) + \sum_{j,k'} C_{jk'}^I I_{j\bar{z}} S_{k'\bar{z}}. \end{aligned} \tag{41}$$

Here the contribution arising from the dipolar and quadrupolar interactions of the S spins has been omitted and the transformations $x \to \bar{z}, y \to \bar{y}, z \to -\bar{x}$ have been used for the I- and S-spin operators.

In the high-temperature approximation, the density matrix in the rotating frame [for time ≥ 0 in Fig. 9(c)] is given by

$$\rho^* \simeq \frac{1}{\mathrm{Tr}(1)} + \frac{\gamma_I \hbar \bar{H}_{1I} I_{\bar{z}} + \gamma_S \hbar \bar{H}_{1S} S_{\bar{z}} - \hbar H_{IS}^*}{k\theta \mathrm{Tr}(1)}, \tag{42}$$

where one has neglected the like spin-spin interaction term in Eq. (41) because of its small associated heat capacity. With $\bar{H}_{1S} = 0$, this equation reduces to the one which has been used to discuss[2] InP multiple-pulse and spin-locking experiments.

The term H_{IS}^* in Eq. (42) establishes thermal contact between the Zeeman and dipolar systems of the I spins and the Zeeman system of the S spins. Equilibrium will be established through mutual spin flip-flop transitions, by pairs of I and S spins. Equations (41) and (42) can be used to calculate the effective energy $E = \mathrm{Tr}(\hbar H_f^* \rho^*)$ and $\bar{Z}$ component magnetization $M_{\bar{z}} = \mathrm{Tr}(\hbar \gamma_I \rho^* I_{\bar{z}})$. The result is

$$E = -(C_I/\theta)[\bar{H}_{1I}^2 + (C_S/C_I)\bar{H}_{1S}^2 + \langle \Delta H^2 \rangle_{IS}] \tag{43}$$

and

$$M_{\bar{z}} = (C_I/\theta)\bar{H}_{1I}. \tag{44}$$

where C_I and C_S are the Curie constants for the I and S spins, respectively. Here, $\langle \Delta H^2 \rangle_{IS} = \mathrm{Tr}(\hbar H_{IS}^*)^2/\mathrm{Tr}(M_{\bar{z}}^2) = 2.56\ \mathrm{G}^2$, which includes the effect attributed to the pseudodipolar interaction between unlike spins as discussed in Sec. II C. In Eq. (43), one has assumed $N_I = N_S$.

If one assumes that the I spins are spin-locked[2] in $\bar{H}_{1I}$ immediately after the application of both rf fields, and also assumes that the lattice spin temperature θ_l is greater than θ, then by conservation of energy and Eq. (44), one obtains

$$M_{\bar{z}}/M_0 = \bar{H}_{1I}^2/[\bar{H}_{1I}^2 + (C_S/C_I)\bar{H}_{1S}^2 + \langle \Delta H^2 \rangle_{IS}]. \tag{45}$$

Equation (45) shows the dependence of the observed echo train signal on the pulse separation and the pulse width of the rf applied to the S spins.

Two typical plots of $M_{\bar{z}}/M_0$ as a function of $\bar{H}_{1I}$ with $\bar{H}_{1S} = 0$ and $\bar{H}_{1S} \neq 0$ are shown in Figs. 10 and 11. Also shown is the theoretical prediction of Eq. (45). The data were taken at both 78 and 4.2 K. In both cases, in order to satisfy Eq. (45), the point $t = 0$ in Fig. 9(c) was chosen at $T' \gtrsim 8\tau$ for $\bar{H}_{1S} = 0$ and $T \lesssim 8\tau$ for $\bar{H}_{1S} \neq 0$. The inequalities establish the criteria for the present multiple-pulse single- and double-resonance analyses, respectively. The poor signal to noise ratio at 78 K for large τ and larger ratio of $t_{\omega_S}/t_{\omega_{S,90°}}$ limits the certainty. The agreement between the predicted equation and the experimental data seems to establish that a common spin temperature can be assigned to the Zeeman and dipolar reservoirs of the I-spin system and the Zeeman term of the S-spin system.

The results suggest that there is an exchange of

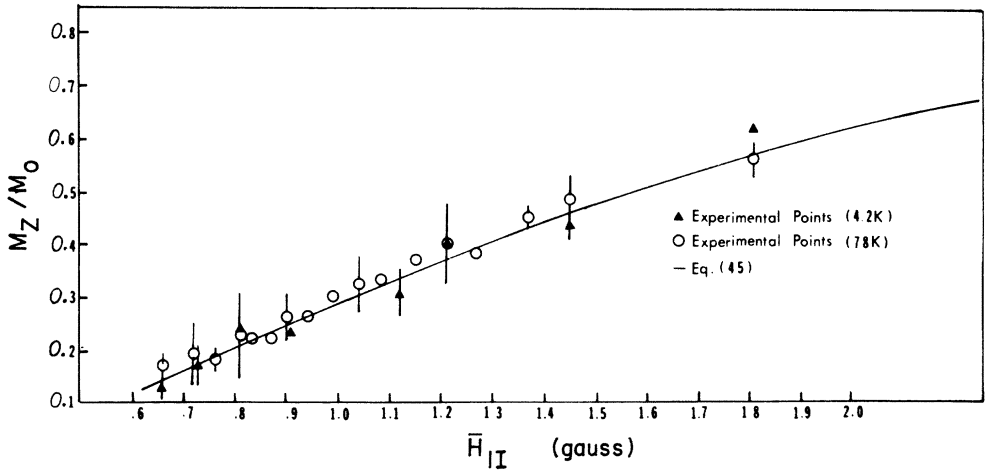

FIG. 10. Magnetization along the effective field in the rotating frame as a function of the rf field with $\bar{H}_{1S} = 0$.

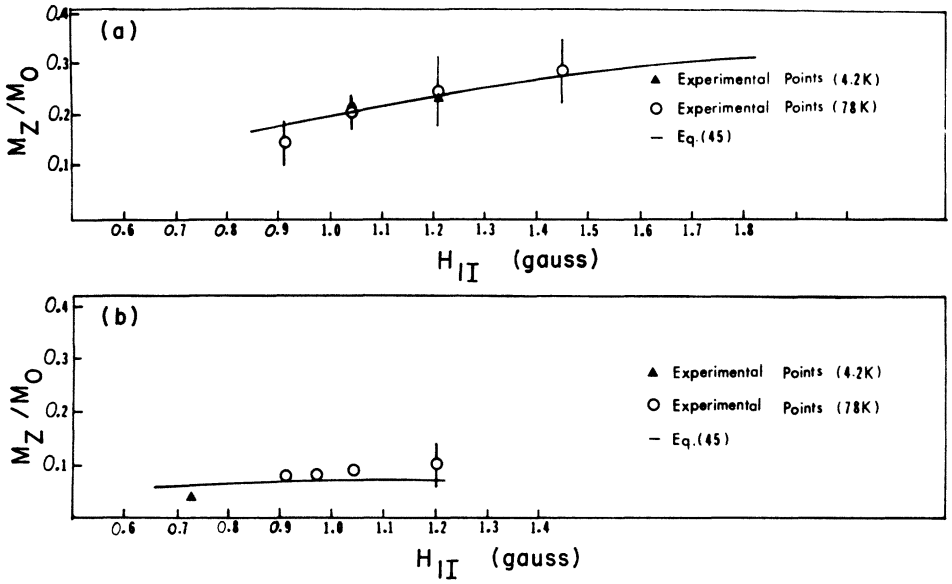

FIG. 11. Magnetization along the effective field in the rotating frame as a function of the rf field with $\bar{H}_{1S} \neq 0$. (a) $t_{\omega_S} \simeq \frac{1}{3} t_{\omega_{S,90°}}$; (b) $t_{\omega_S} \simeq t_{\omega_{S,90°}}$.

energy between the Zeeman and dipolar reservoirs of the I spins and the Zeeman reservoir of the S spins via the mutual coupling between unlike spins. It is now proposed that a cross-relaxation model be adopted, based on our multiple-pulse double-resonance experiments to simulate the mechanical rotation experiments, and used to interpret the increase in T_1 and the plateau in the rotating sample experiment shown in Fig. 8.

One can view the various terms in Eq. (41) as energy reservoirs. On the other hand, the multiple pulses, applied to both I and S spins, can be viewed as a kind of artificial line-narrowing mechanism. They have been regarded as a "discrete step rotations" by Mansfield.[13] For simplicity, the following discussion will presume that rotating rf fields are continuously applied to both I and S spins.

In the rotating frame, with $\bar{H}_{1S} = 0$, the Zeeman energy reservoir of the S spins is at infinite temperature, since $\vec{M}_S$ is perpendicular to $\vec{H}_{1S}$ in this frame. The I spins, which experience a $90 - \tau - 90_{90} - 2\tau - 90_{90} - 2\tau \cdots$ pulse sequence, will be at lower spin temperature since the I spins are assumed to be spin locked. It follows that there will be a heat flow from the Zeeman system of the S spins to the rest of the energy reservoirs via cross relaxation as is illustrated in Fig. 12. There, T_{1I}, T_{1S} are the respective spin-lattice relaxation times of the spin systems and R_{SI}, R_{IS} are, respectively, the rates of energy flow from the S-spin system to the I-spin system and vice versa.

Based on a cross-relaxation model similar to that shown in Fig. 12 and assuming the two spin systems (characterized by the spin temperatures θ_I and θ_S, respectively) to be interacting weakly with each other and with the lattice, Schumacher[59] obtained differential equations governing the time rate of change of the spin temperatures θ_I and θ_S. The solutions to these differential equations were[59]

$$1/\theta_I = Ae^{m_+ t} + Be^{m_- t} + C\,, \qquad 1/\theta_S = A'e^{m_+ t} + B'e^{m_- t} + C'\,. \tag{46}$$

Here A, B, C depend on the initial conditions and A', B', and C' are determined by the differential equations. Where

$$m_\pm = -(1/2T_{1I})[1 + g + (1+\mu)h \pm S']\,, \tag{47a}$$

with

$$\mu = R_{SI}/R_{IS} = T_{IS}/T_{SI}\,, \tag{47b}$$

$$g = T_{1I}/T_{1S}\,, \quad h = R_{IS}/R_1 = T_{1I}/T_{IS}\,, \tag{47c}$$

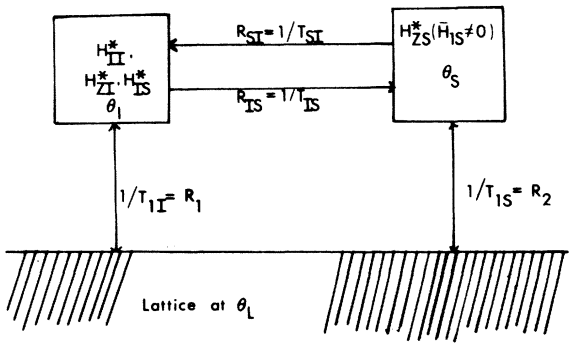

FIG. 12. Cross-relaxation model adopted for AlP.

$$S' = [(g-1)^2 + (\mu+1)^2 h^2 + 2h(\mu-1)(g-1)]^{1/2} . \tag{47d}$$

Since $m_+ < m_-$, one assumes that, for $h \neq 0$, $1 - M_Z/M_0 \propto e^{m_- t}$. The spin-lattice relaxation rate of the I system is then defined as

$$1/T_{1I}(\omega) = -m_- , \tag{48}$$

with m_- given in Eqs. (47).

Lurie and Slichter[56] calculated the cross-relaxation rates R_{1S} and R_{SI} in the rotating frame, based on a cross-relaxation model similar to our Fig. 12 but without taking the spin-lattice interactions into consideration. They calculated the transition probability assuming the cross-coupling term between the I and S systems to be the perturbation. Their results for $H_{1I} \geq H_L$ (H_L is the local field) with $\bar{\omega}_I = \bar{\omega}_S$ can be slightly modified to

$$R_{IS} = \frac{1}{T_{IS}} = \frac{S(S+1)}{I(I+1)} \times R_{SI} \frac{1}{1 + (\frac{1}{3}\langle \Delta H^2 \rangle_{II} + \langle \Delta H^2 \rangle_{IS})(16\gamma_I^2/\pi^2)\tau^2} , \tag{49a}$$

$$R_{SI} = 1/T_{SI} = \tfrac{4}{3}(\gamma_S/\gamma_I)^2 (\tfrac{1}{10}\pi \langle \Delta\omega^2 \rangle_{II})^{1/2} , \tag{49b}$$

$$\bar{\omega}_I = \gamma_I \bar{H}_{1I} , \quad \bar{\omega}_S = \gamma_S \bar{H}_{1S} . \tag{49c}$$

Also, for later discussion, one rewrites Eq. (47b) as

$$\mu = R_{SI}/R_{IS} = T_{IS}/T_{SI} = \frac{I(I+1)}{S(S+1)} \left(1 + \frac{16\gamma_I^2}{\pi^2} (\langle \Delta H^2 \rangle_{IS} + \tfrac{1}{3}\langle \Delta H^2 \rangle_{II})\right)\tau^2 . \tag{50}$$

In the following discussion let us accept these equations as representing the cross relaxation rates at $\bar{\omega}_I = \bar{\omega}_S$.

From Eq. (49a), one sees that as τ is increased, the rate $R_{\pm I}$ is decreased, thus T_{IS} is increased. The increase in τ corresponds to slower sample rotation and the cross-relaxation time T_{IS} increases as the rotation becomes slower. It is interesting to note that, as $\tau \to \infty$, which corresponds to the static case in the rotating sample experiment, one has $T_{IS} \to \infty$. That is, in the static case, it is difficult to establish cross relaxation between the two spin systems since one of the cross-relaxation times approaches infinity. The two spin systems then interact with the lattice independently as far as spin-lattice relaxation is concerned. One could rewrite Eq. (47a) as

$$\frac{d(-m_-)}{dh} = \frac{1}{2T_{1I}} \frac{4\mu(g-1)^2}{S'^2(1+\mu) + S'[h(1+\mu)^2 + (\mu-1)(g-1)]} \tag{51a}$$

and Eq. (47d) as

$$S' = \{[(g-1) + (\mu-1)h^2] + 4\mu h^2\}^{1/2} . \tag{51b}$$

From Eqs. (51) and (48), one sees that $T_{1I}(\omega)$ increases as τ decreases, which corresponds to faster rotation in the rotating sample experiments (see Fig. 8). It seems reasonable to assume that, in the laboratory frame rotating sample experiments, there also exists a cross-relaxation phenomenon, analogous to the situation in the rotating frame multiple-pulse double-resonance experiments.

One knows that as τ is decreased, $T_{1I}(\omega)$ increases. A limiting value can be obtained if one sets $dm_-/dh = 0$. One then gets

$$1/T_{1I}(\omega) = -m_- = (1/2T_{1I})(1+k) + (1/2T_{1S})(1-k) , \tag{52a}$$

with

$$k = (\mu-1)/(\mu+1) , \tag{52b}$$

where T_{1I}, T_{1S} are the static spin-lattice relaxation times of the I and S spins, respectively. Let $\tau \to 0$, which corresponds to $\bar{\omega}_I = \bar{\omega}_S \to \infty$ [from Eqs. (37)–(39) and (49c), i.e., corresponds to very high sample rotation frequency]. From Eq. (50), one gets

$$\mu \to I(I+1)/S(S+1) = \tfrac{3}{35} \ll 1 .$$

Then, $K \to -1$ and from Eq. (52a), one obtains $T_{1I}(\omega) \to T_{1Al}$. That is, as the rotation frequency is increased to some limit, where spin diffusion no longer plays an important role, the spin-lattice relaxation time of phosphorous will be limited by the rotationally invariant spin-lattice relaxation times of aluminum via the cross relaxation between the ^{31}P and ^{27}Al in AlP.

IV. SUMMARY

The mutual second moment of the ^{31}P nuclei in AlP, which is deduced from the FID and solid echo experiments, is found to be 20% smaller than the purely dipolar value. This reduction in second moment is interpreted in terms of an interference effect of the pseudodipolar interaction. The negative sign of the pseudodipolar interaction constant is in agreement with the prediction of the localized bond model. An additional line broadening in the ^{27}Al resonance probably arises from first-order quadrupolar interaction with unresolved satellites. Nuclear relaxation of Al^{31}P arises from paramagnetic centers, particularly at higher temperatures. A cross-relaxation model, which is based on multiple-pulse double-resonance experiments in the rotating frame, can be used to describe one of the results of earlier experiments on rotating samples of AlP.

†Research supported by the Air Force Office of Scientific Research and the National Science Foundation.

*Present address: Department of Physics, Iowa State University, Ames, Ia.

[1]R. L. Melcher, *Semiconductors and Semimetals*, edited by R. K. Willardson and A. G. Beer (Academic, New York, 1966), Vol. II, Chap. 7.
[2]M. Engelsberg and R. E. Norberg, Phys. Rev. 5, 3395 (1972).
[3]R. K. Hester, A. Sher, and J. F. Soest, Phys. Rev. B 10, 4262 (1974).
[4]R. K. Sundfors, Phys. Rev. 185, 458 (1969).
[5]M. M. Ruderman and C. Kittel, Phys. Rev. 96, 99 (1954).
[6]N. Bloembergen and T. J. Rowland, Phys. Rev. 97, 1679 (1955).
[7]P. W. Anderson, Phys. Rev. 99, 623 (1955).
[8]M. H. Cohen and F. Reif, Solid State Phys. 5, 321 (1957).
[9]A. N. Gusatinskii and S. A. Nemnonov, in *Collection: Thermodynamics and Chemical Binding in Semiconductors*, edited by N. N. Sirota (Consultants Bureau, New York, 1968).
[10]J. R. Van Wazer, *Phosphorous and Its Compounds* (Interscience, New York, 1958), Vol. I.
[11]H. Kessemeier and R. E. Norberg, Phys. Rev. 155, 321 (1967).
[12]P. Mansfield and D. Ware, Phys. Lett. 23, 421 (1966).
[13]P. Mansfield and D. Ware, Phys. Lett. 22, 133 (1966).
[14]J. S. Waugh and C. H. Wang, Phys. Rev. 162, 209 (1967).
[15]S. R. Hartmann and E. L. Hahn, Phys. Rev. 128, 2042 (1962).
[16]I. J. Lowe and R. E. Norberg, Phys. Rev. 107, 43 (1957).
[17]J. G. Powles and H. G. Strange, Proc. Phys. Soc. Lond. 82, 6 (1963).
[18]P. Mansfield, Phys. Rev. 137, A961 (1965).
[19]J. H. Van Vleck, Phys. Rev. 74, 1168 (1948).
[20]S. Clough and W. I. Goldburg, J. Chem. Phys. 45, 4080 (1966).
[21]K. Yosida and T. Moriya, J. Phys. Soc. Jpn. 11, 33 (1956).
[22]N. Bloembergen and P. P. Sorokin, Phys. Rev. 110, 865 (1958).
[23]M. Engelsberg, Ph.D. thesis (Washington University, 1971) (unpublished).
[24]Y. S. Hwang, Ph.D. thesis (Washington University, 1975) (unpublished).
[25]W. A. Harrison, Phys. Rev. B 8, 4487 (1973).
[26]C. Huang, J. A. Moriarty, A. Sher, and R. A. Breckenridge, Phys. Rev. B 12, 5395 (1975).
[27]C. Huang, J. A. Moriarty, and A. Sher (unpublished).
[28]E. H. Rhoderick, Philos. Mag. 3, 545 (1958).
[29]E. H. Rhoderick, J. Phys. Chem. Solids 8, 498 (1958).
[30]D. J. Oliver, J. Phys. Chem. Solids 11, 257 (1959).
[31]A. Abragam, *The Principles of Nuclear Magnetism* (Oxford U.P., London, 1961).
[32]K. Kambe and J. F. Ollom, J. Phys. Soc. Jpn. 11, 50 (1956).
[33]E. Fermi and E. Segrè, Z. Phys. 82, 729 (1933).
[34]N. Bloembergen, Physics (Utr.) 20, 1130 (1954).
[35]G. L. Pearson and J. Bardeen, Phys. Rev. 75, 865 (1949).
[36]R. C. Fletcher, W. A. Yager, G. L. Pearson, A. H. Holden, W. T. Reed, and F. R. Meritt, Phys. Rev. 94, 1392 (1954).
[37]G. R. Khutsishvili, Prog. Low Temp. Phys. 6, 375 (1960).
[38]H. E. Rorschach, Jr., Physica (Utr.) 30, 38 (1964).
[39]P. G. de Gennes, J. Phys. Chem. Solids 7, 345 (1958).
[40]G. R. Khutsishvili, Zh. Eksp. Teor. Fiz. 43, 2179 (1962) [Sov. Phys.-JETP 16, 1540 (1963)].
[41]G. R. Khutsishvili, Usp. Fiz. Nauk 87, 211 (1965) [Sov. Phys.-Usp. 8, 743 (1966)].
[42]W. E. Blumberg, Phys. Rev. 119, 79 (1960).
[43]A. G. Akhmedov and R. A. Dautov, Fiz. Tverd. Tela 6, 529 (1964) [Sov. Phys.-Solid State 6, 415 (1964)].
[44]P. Mansfield and D. Ware, in *Colloque Ampere XIV*, edited by R. Bline (North-Holland, Amsterdam, 1967).
[45]W. I. Goldburg and M. Lee, Phys. Rev. Lett. 11, 255 (1963).
[46]D. Barnaal and I. J. Lowe, Phys. Rev. Lett. 11, 258 (1963).
[47]D. C. Look and I. J. Lowe, J. Chem. Phys. 44, 2995 (1966).
[48]P. Mansfield and D. Ware, Phys. Rev. 168, 318 (1968).
[49]P. Mansfield, K. H. B. Richards, and D. Ware, Phys. Rev. B 1, 2048 (1970).
[50]D. A. McArthur, E. L. Hahn, and R. E. Walstedt, Phys. Rev. 188, 609 (1969).
[51]J. Okada and R. Kado, J. Phys. Soc. Jpn. 32, 1412 (1972).
[52]R. E. Walstedt, D. A. McArthur, and E. L. Hahn, Phys. Lett. 15, 7 (1965).
[53]D. A. McArthur, Ph.D. thesis (University of California at Berkeley, 1967) (unpublished).
[54]D. V. Lang and P. R. Moran, Phys. Rev. B 1, 53 (1970).
[55]P. R. Spencer, H. D. Schmid, and C. P. Slichter, Phys. Rev. 1, 2989 (1970).
[56]F. M. Lurie and C. P. Slichter, Phys. Rev. 133, A1108 (1964).
[57]Y. Tsutsumi, M. Kunitomo, and T. Hashi, J. Phys. Soc. Jpn. 20, 2095 (1965).
[58]P. Mansfield and G. P. Grant, Phys. Lett. A 33, 130 (1970).
[59]R. T. Schumacher, Phys. Rev. 112, 837 (1958).

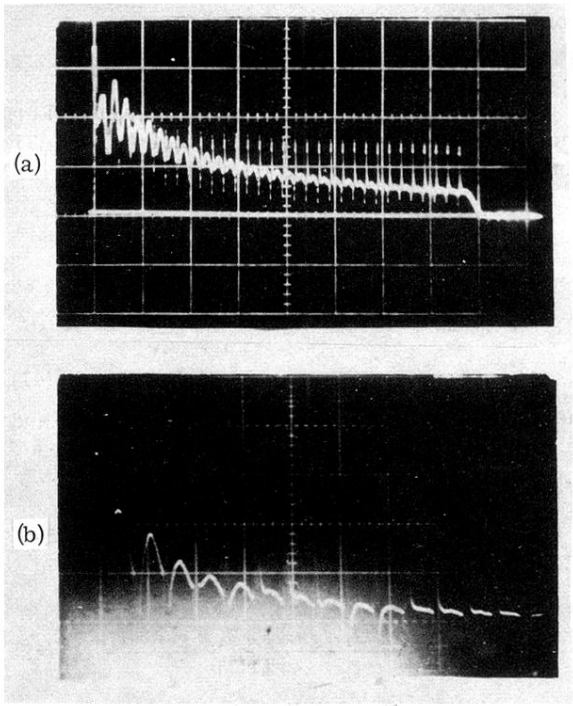

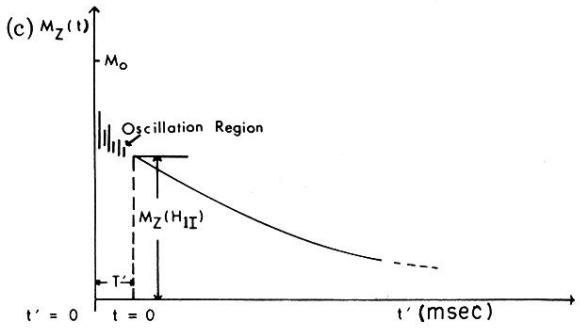

FIG. 9. (a) Oscilloscope photograph of train of solid echoes in the multiple-pulse single-resonance experiment ($\overline{H}_{1S}=0$). τ is 60 μsec and the sweep length is 5 msec. (b) Echo train in multiple-pulse double-resonance experiment ($\overline{H}_{1S}\neq 0$). τ is 60 μsec and the sweep length is 2 msec. (c) Sketch of the evolution of the magnetization $M_Z(\overline{H}_{1I})$ of the I spins for typical values of $\overline{H}_{1I}$.